JOURNAL OF MATERIALS SCIENCE 17 (1982) 741–746

A model for the stress–strain behaviour of toughened polystyrene

Part 1

S. D. SJOERDSMA, D. HEIKENS
Eindhoven University of Technology, Laboratory for Polymer Technology, P.O. Box 513, 5600 MB Eindhoven, The Netherlands

A model has been developed to determine the rates of craze initiation and craze growth in opaque materials that deform by crazing, such as toughened polystyrene, and to predict their stress–strain behaviour. It is shown that crazed polystyrene toughened with low density polyethylene can be regarded as a series of linearly elastic crazes and toughened polystyrene. This implies that the amount of craze material, stress and strain are related in a simple fashion. As the amount of craze material can be calculated from the rates of craze initiation and craze growth, stress–time behaviour can be calculated if strain–time behaviour is known, and vice versa.

1. Introduction

The stress–strain behaviour of polymers that deform by crazing has been modelled by a number of authors [1–7]. In general their method was based on an adaption of the Johnston–Gilman theory for dislocation dynamics [8, 9]. Craze growth rates were determined microscopically and combined with the Johnston–Gilman theory to obtain a relationship that describes stress–strain properties. This approach is obviously not feasible for rubber-toughened materials like toughened polystyrene (TPS) as the crazing process cannot be followed microscopically due to the opacity of these materials. Furthermore, the use of the Johnston–Gilman theory implies that crazing is regarded as a purely plastic process, while in fact the strain of a crazed sample is largely elastic. This can be concluded from the large decrease in strain of a crazed TPS upon removal of stress (see Fig. 1). These considerations induced the present authors to attempt a different approach to describe the stress–strain behaviour of polymers that deform by crazing.

In the underlying study a new model of stress–strain behaviour is formulated, applications of this model on polystyrene–polyethylene (PS–PE) blends will be presented in a subsequent paper [10].

2. Theory

2.1. Deformation characteristics of toughened polystyrene

If toughened polystyrene (TPS) is subjected to a tensile test generally stress-whitening and yielding will be observed [11, 12]. Both phenomena are consequences of crazing. Many details concerning crazing are given in a number of comprehensive reviews [13–16]. Only the aspects related directly with the stress–strain behaviour will be discussed here briefly.

The crazing process can be divided into three steps, initiation, growth and termination [17]. The rates of craze initiation and growth are stress dependent: as the stress increases, during, for instance, a constant strain rate tensile test, crazes will be initiated and will grow, causing stress whitening. At yield point these rates are so high that for further elongation of the sample no further stress increase is necessary, in effect less is needed to maintain the elongation rate imposed on the sample by the tensile tester [18]. This stress decrease lowers the rates of craze initiation and craze growth. Consequently the stress does not drop to zero but becomes approximately constant at a rather high level (see Fig. 1). At this stage craze termination due to, for instance, local creep [19] or a decrease in the craze initiation rate as

0022–2461/82/030741–06$03.22/0

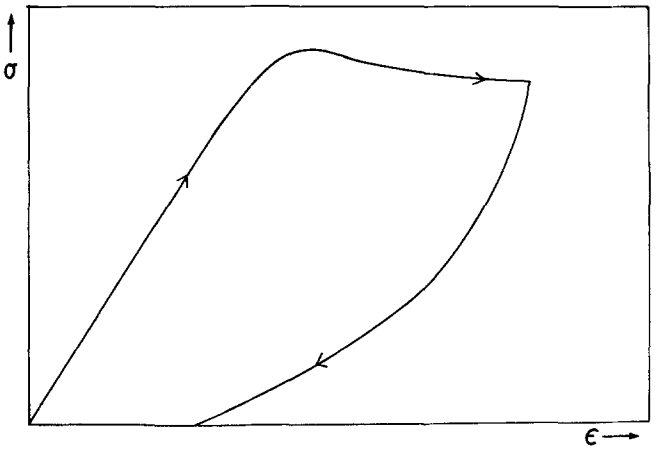

Figure 1 Stress–strain response of PE toughened PS in a constant stress-rate experiment. The strain decrease is caused by reversing the movement of the tensile tester.

observed for surface crazes in homopolymers [20, 21] during constant stress experiments, may become important.

During a tensile test the fibrils spanning the crazes will be stressed and will increase in length by surface drawing [22, 23]. If now the strain is reduced, a rapid fall in stress takes place (see Fig. 1). Initially the stress on the fibrils will diminish, causing a decrease in elastic craze strain. This decrease will be small due to the high modulus of the fibrils. However, the elastically deformed surroundings of the crazes cause further closure of the crazes, resulting in buckling of the craze fibrils and a strong decrease in craze strain [24].

2.2. Modelling of the stress–strain behaviour

In order to model the stress–strain behaviour a more quantitative analysis is needed than that given in the preceding section.

The morphology of crazed TPS is such that this material can be regarded as uncrazed TPS connected in series with polystyrene (PS) crazes [18]. The length of a sample after it has been subjected to a tensile test can then be expressed as the sum of the length of TPS and of the crazes.

The amount of PS that is converted into fibrillar craze material can be calculated from the (stress–dependent) rates of craze initiation and growth. If the PS content of the crazes is known then this content can be combined with the amount of PS that has been converted into craze material, which allows the calculation of the total volume occupied by crazes. As the cross-sectional area of TPS that is subjected to a tensile test is nearly constant [16] this volume can be converted directly into sample strain due to craze strain. In this way the rates of craze initiation and growth can be related with craze strain, which forms the basis of the model.

2.3. Elaboration of the model

While the length of a crazed sample in principle can be modelled as the sum of the lengths of TPS and crazes, a refinement is needed in order to account for the effects of stress. It has already been noted that three forces are acting within a stressed tensile specimen: the retractive forces of the elastically strained TPS and craze fibrils, and the craze closing forces exerted by the elastically deformed surroundings of the crazes. The stress–strain response in the absence of craze growth can then be represented in a simple fashion by a three-spring model. Two springs are parallel, representing the retractive forces exerted by the elastically strained craze fibrils and by the elastically deformed surroundings of the crazes. A third spring connected in series with the set of the two parallel springs is needed to represent the retractive force exerted by the elastically strained TPS. Craze growth can be incorporated by such a model by allowing a length increase of the spring that represents the elastically strained craze fibrils (increase of the amount of crazed material) at the expense of the length of the spring that represents the elastically strained TPS.

This three-spring model can be used to develop a relationship that describes stress–strain behaviour of TPS for both positive and negative strain rates as the effect of buckling of the craze fibrils can be taken into consideration. Here a more simple approach is chosen by confining the stress–strain model to tensile tests during which no buckling of the craze fibrils takes place, or, consequently,

during which little or no decrease of sample strain takes place. This means, in terms of the three-spring model, that the set of parallel springs can be replaced by one spring, allowing a simple treatment of the effect of stress on the length of the tensile specimen.

Furthermore, for simplicity, changes in the cross-sectional area of a sample during tensile deformation will be neglected as it can be shown that these changes never exceed 1% [16]. Assume that v cm^3 PS per cm^3 TPS have been converted into craze fibrils, then the length of the crazed specimen, l_{TPS} can be represented by

$$l_{TPS} = \frac{V_0 - V_0 v}{A_0} = l_0(1-v), \qquad (1)$$

where V_0, A_0 and l_0 are respectively the volume, the area of the cross-section and the length of the original uncrazed tensile specimen.

Further, if the volume-fraction of PS within a craze at zero stress on the fibrils is f^{-1} (cm^3 PS/cm^3 craze), where f is the expansion factor, then the length of craze fibrils at zero stress on the fibrils, l_c is given by

$$l_c = \frac{fV_0 v}{A_0} = fvl_0. \qquad (2)$$

As linear tensile elasticity is a good approximation for the stress–strain behaviour of non-crazed TPS, and assuming the same for the crazes provided the craze fibrils are stressed elastically, then Equations 1 and 2 may be combined to obtain

$$l = l_0(1-v)\left(1+\frac{\sigma}{E_{TPS}}\right) + vfl_0\left(1+\frac{\sigma}{E_{cr}}\right), \qquad (3)$$

which can be rearranged as follows

$$v = \frac{1 - l_0\left(1+\frac{\sigma}{E_{TPS}}\right)}{f\left(1+\frac{\sigma}{E_{cr}}\right) - \left(1+\frac{\sigma}{E_{TPS}}\right)} l_0^{-1}, \qquad (4)$$

or

$$v = \frac{\epsilon - \frac{\sigma}{E_{TPS}}}{f\left(1+\frac{\sigma}{E_{cr}}\right) - \left(1+\frac{\sigma}{E_{TPS}}\right)}, \qquad (5)$$

where E_{TPS} is the tensile modulus of TPS, E_{cr} is the tensile modulus of the craze fibrils combined with the effect of the closing forces, σ and ϵ are stress and strain respectively. In Equation 5 the volume-fraction of PS converted into craze fibrils, v, is expressed with only stress and strain as variables. Using this relationship v can be calculated at any stress–strain situation if the expansion factor f and the moduli E_{TPS} and E_{cr} are known. Furthermore, v can be calculated from the rates of craze initation and growth [25]: from the lack of changes in the cross-sectional area of a specimen during a tensile test, apart from a small Poisson ratio effect, it can be concluded that PS transport from the bulk to the crazes takes place only in the direction of the applied stress.

If now k_g is defined as the rate of the surface drawing process that results in this transport then $\int_\tau^t k_g(\tau)\,d\tau$ denotes the increase in length at time, t, of a fibril that originated at a time, τ. Further, if k_i is the rate of craze surface formation normal to the stress direction per unit volume TPS, then

$$v = \frac{1}{f}\int_0^t k_i(\tau)\int_\tau^t k_g(\tau)\,d\tau\,d\tau. \qquad (6)$$

Equations 4, 5 and 6 can be combined to obtain a general stress–strain relationship, i.e.,

$$\frac{1}{f}\int_0^t k_i(\tau)\int_\tau^t k_g(\tau)\,d\tau\,d\tau = \frac{1 - l_0(1+\sigma/E_{TPS})}{f(1+\sigma/E_{cr}) - (1+\sigma/E_{TPS})} l_0^{-1}, \qquad (7)$$

or

$$\frac{1}{f}\int_0^t k_i(\tau)\int_\tau^t k_g(\tau)\,d\tau\,d\tau = \frac{\epsilon - \sigma/E_{TPS}}{f(1+\sigma/E_{cr}) - (1+\sigma/E_{TPS})}. \qquad (8)$$

As it may be assumed that k_i and k_g are dependent only on stress and time (at constant temperature) Equations 7 and 8 can be used to determine the stress–time behaviour if the strain–time behaviour is known and vice versa.

3. Experimental procedure

By dilatometric measurements at ambient temperature on PS–PE blends it was found that a ratio of 85 to 15 wt % PS to lowest density (ld) PE blend deforms only by crazing [26, 27]. Therefore this blend was chosen to verify the model set forth in this paper. The polystyrene used was Styron 634 ($\bar{M}_n \sim 10^5$, $\bar{M}_w/\bar{M}_n \sim 2.5$), obtained from Dow Chemical Co., the low density polyethylene was Stamylan 1500 ($\bar{M}_n \sim 3.5\ 10^4$, $\bar{M}_w/\bar{M}_n \sim 30$) from DSM, Netherlands. Blends were prepared by melt mixing on a Schwabenthan laboratory mill. To improve bulk mixing the polymer sheet was

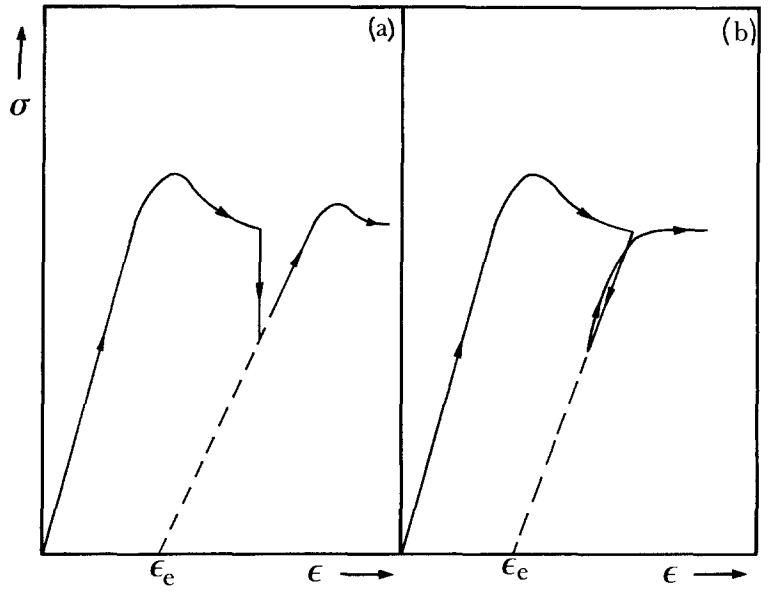

Figure 2 Determination of ϵ_e by (a) a stress-relaxation experiment (b) reversing the movement of the tensile tester.

turned 90° every minute. Tensile specimens in accordance with ASTM D 638 III were machined from compression moulded sheets, and were conditioned at 21° C and 65% relative humidity (r.h.) for at least 48 hours. Constant strain-rate tensile tests were performed on an Instron tensile tester, constant stress tests using dead loads. The strain was measured directly using an HBM linear voltage displacement transducer and amplifier.

4. Results and discussion

4.1. Validity of the series model: determination of the craze modulus and the expansion factor

The applicability of the series model can be verified by comparing the strain of a crazed specimen under stress with the strain that the same sample would have under zero stress, assuming that no buckling of the craze fibrils takes place. This also allows the evaluation of the craze modulus and of the expansion factor.

If the series model is valid and if no craze fibril buckling takes place then the length of a crazed sample extrapolated to zero stress, l_e, equals (from Equations 1–3)

$$l_e = l_{TPS} + l_{cr} = l_0(1-v) + l_0 vf, \quad (9)$$

or

$$\epsilon_e = vf - v. \quad (10)$$

Now, using Equations 9 and 10, v can be expressed in terms of ϵ_e, and by inserting the result in Equation 3 the following relationship between ϵ and ϵ_e is obtained, i.e.,

$$\epsilon = \epsilon_e\left[1 + \frac{\sigma}{f-1}\left(\frac{f}{E_{cr}} - \frac{1}{E_{TPS}}\right)\right] + \frac{\sigma}{E_{TPS}}. \quad (11)$$

So, if the series model is valid, a plot of ϵ against ϵ_e should result in a straight line, with a slope from which a mathematical relation between f and E_{cr} can be derived. Therefore ϵ_e has been determined in two ways by extrapolation.

If during a constant strain rate test the strain rate is reduced to zero then stress relaxation takes place (see Fig. 2a). Crazes still initiate and grow, causing a stress decrease until the stress has fallen so low that both initiation and growth have stopped. For the 85–15 PS–ldPE blend this stress was 9.1 MPa, independent of the strain rate. In this situation the stress on the fibrils must be small or zero but no buckling will take place. If the tensile tester is started again the stress increases almost linearly until it reaches such a level that crazes start to grow again and are being initiated. Extrapolation of this linear stress–strain response to zero stress gives ϵ_e.

A second way of determining ϵ_e is a sudden reverse of the movement of the tensile test during a constant strain rate tensile test (see Fig. 2b). If this is done fast enough then initially the resulting stress decrease is linear with strain as hardly any craze growth can take place. This linear response again makes extrapolation to zero stress possible, providing ϵ_e.

The results of both methods are consistent.

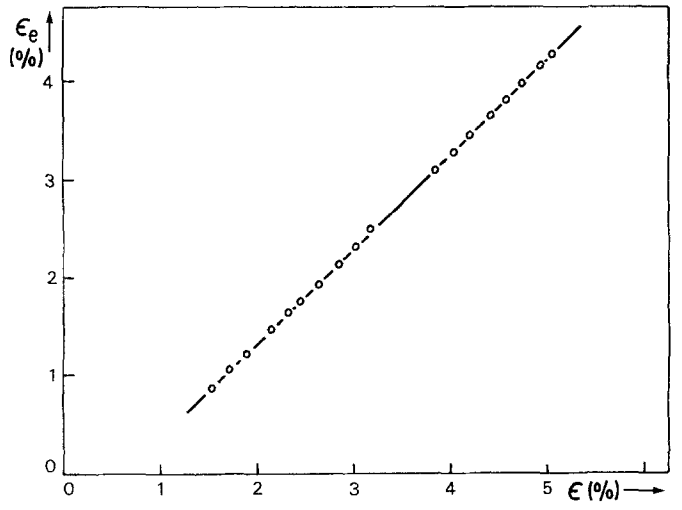

Figure 3 The linear dependence of ϵ_e on ϵ proves the applicability of a linear elastic series model.

As shown in Fig. 3 a linear relationship between ϵ_e and ϵ is indeed obtained, showing the applicability of the linear elastic series model. The following relation between E_{cr} and f was obtained:

$$E_{cr} = \frac{1000}{2.9 - \frac{2.4}{f}} . \qquad (12)$$

Electron microscopy and optical microscopy work on stressed PS crazes resulted in values for f ranging from 3 to 6, averaging 4 [23, 28, 29]. Using the average value for f the apparent craze modulus was calculated to be 410 MPa.

4.2. Time dependence of the rates of craze initiation and growth

The possible time dependence of the craze area formation normal to the stress direction can be evaluated by performing an Avrami-type of analysis [25, 30]. It can be shown from Equation 6 that v should increase with the square of time during a constant stress experiment if k_i and k_g are time-independent. Plots of ln v, as calculated using Equations 4 and 5 against ln t have a slope of 1.6. This value is independent of the applied stress, and thus independent of the duration of the experiment. Evidently k_i and k_g are not time-dependent. The fact that the slope is somewhat less than 2 arises from the initiation of crazes that takes place during the application of stress at the beginning of the constant stress experiment. This initiation is indicated by the positive slope of a plot of v against t immediately after the beginning of the experiment.

The time dependence of v can now be expressed as the sum of two terms. The first is craze initiation

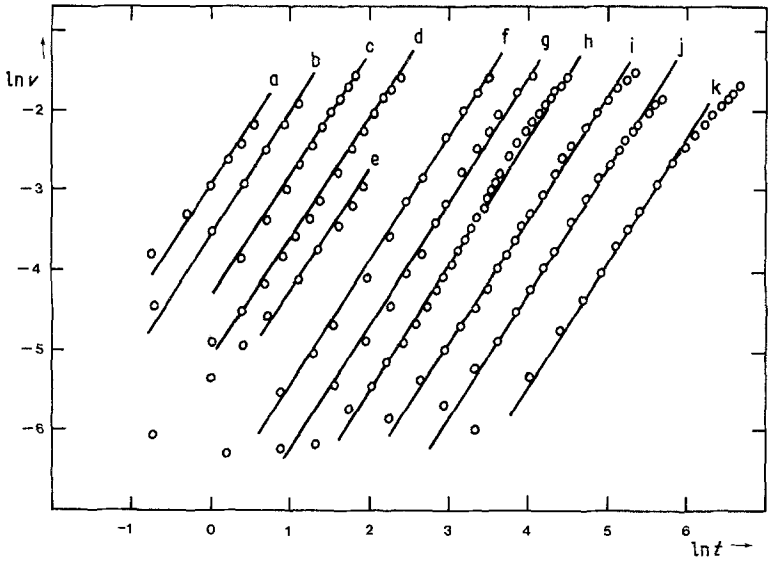

Figure 4 Plots of ln v against ln t as determined during creep experiments, which indicate that k_i and k_g are not time-dependent. The applied stresses in MPa are a, 23.4; b, 22.2; c, 21.3; d, 20.3; e, 19.1; f, 17.9; g, 17.1; h, 16.2; i, 15.2; j, 14.4; k, 13.6.

and growth during the experiment, and is proportional to the square of time. The second term arises from growth of the crazes that were initiated during the application of stress and is only proportional to time, which explains the fact that the value of the slope of ln v against ln t is somewhat lower than 2. The time-dependence of v at high strain is not taken into consideration because of craze-termination effects that are neglected in this model.

5. Conclusion

As k_i and k_g are dependent on stress only Equation 6 can be differentiated twice with respect to time to obtain:

$$\frac{1}{f}k_i k_g = -\frac{1}{k_g}\frac{dk_g}{d\sigma}\frac{d\sigma}{dt}\frac{dv}{dt}+\frac{d^2v}{dt^2}. \quad (13)$$

Differentiating Equation 5 and inserting the results in Equation 13 results in the stress–strain equation in differential form

$$\frac{1}{f}k_i k_g = \frac{1}{p\sigma+r}\left[\frac{d\sigma}{dt}\left(\frac{1}{k_g}\frac{dk_g}{d\sigma}+\frac{2p}{p\sigma+r}\right)\times\left(\frac{d\sigma}{dt}\frac{p\epsilon+r/E_{TPS}}{p\sigma+r}-\frac{d\epsilon}{dt}\right)+\frac{d^2\epsilon}{dt^2}-\frac{p\epsilon+r/E_{TPS}}{p\sigma+r}\frac{d^2\sigma}{dt^2}\right], \quad (14)$$

where p and r are constants, defined as follows:

$$p = \frac{f}{E_{cr}}-\frac{1}{E_{TPS}} \quad (15)$$

and

$$r = f-1. \quad (16)$$

As p and r can be determined or are known from literature, only the rates of craze initiation and craze growth have to be known to determine the stress during any strain programme or the strain during any stress programme by solving Equation 14. Furthermore this equation can be used to determine the craze initiation and growth rates from known stress–strain behaviour.

In a subsequent paper it will be shown how these rates can be determined from constant stress rate and constant strain rate experiments by employing Equation 14. Using values for k_i and k_g thus obtained, stress–strain behaviour can be predicted using the model.

Acknowledgements

The authors wish to thank Mr A. C. A. M. Bleijenberg for helpful discussions.

Received 3 June
and accepted 24 July 1981

References

1. N. BROWN, *J. Polymer Sci. Polymer Phys. Ed.* **11** (1973) 2099.
2. N. BROWN and S. FISCHER, *ibid.* **13** (1975) 1315.
3. N. BROWN, *Phil. Mag.* **32** (1975) 1041.
4. Y. IMAI and N. BROWN, *J. Polymer Sci. Polymer Phys. Ed.* **14** (1976) 723.
5. N. BROWN, B. METZGER and Y. IMAI, *ibid.* **16** (1978) 1085.
6. M. KITAGAWA and M. KAWAGOE, *ibid.* **17** (1979) 663.
7. J. B. C. WU and N. BROWN, *J. Rheol.* **23** (1979) 231.
8. W. G. JOHNSTON and J. J. GILMAN, *J. Appl. Phys.* **30** (1958) 129.
9. J. J. GILMAN, *ibid.* **44** (1973) 675.
10. S. D. SJOERDSMA and D. HEIKENS, *J. Mater. Sci.* **17** (1982) 747.
11. E. H. MERZ, G. C. CLAVER and M. BAER, *J. Polymer Sci.* **22** (1956) 325.
12. C. B. BUCKNALL and R. R. SMITH, *Polymer* **6** (1965) 437.
13. R. P. KAMBOUR, *Macromol. Rev.* **7** (1973) 1.
14. S. RABINOWITZ and P. BEARDMORE, *CRC Crit. Revs. Macromol. Sci.* **1** (1972) 1.
15. W. RETTING, *Angew. Makromol. Chem.* **58/59** (1977) 133.
16. C. B. BUCKNALL, "Toughened Plastics" (Applied Science Publishers, London, 1977).
17. O. K. SPURR and W. D. NIEGISCH, *J. Appl. Polymer Sci.* **6** (1962) 585.
18. J. HOARE and D. HULL, *Phil. Mag.* **26** (1972) 443.
19. R. P. KAMBOUR and R. E. ROBERTSON, in "The Mechanical Properties of Plastics", edited by A. D. Jenkins (North Holland Publishing Co., Amsterdam, 1972) p. 607.
20. A. S. ARGON and J. G. HANNOOSH, *Phil. Mag.* **5** (1977) 1195.
21. M. KITAGAWA, *J. Polymer Sci. Polymer Phys. Ed.* **17** (1979) 663.
22. P. BEAHAN, M. BEVIS and D. HULL, *J. Mater. Sci.* **8** (1972) 162.
23. B. D. LAUTERWASSER and E. J. KRAMER, *Phil. Mag.* **A39** (1979) 469.
24. M. J. DOYLE and J. G. WAGNER, *Adv. Chem. Series* **154** (1976) 63.
25. M. AVRAMI, *J. Chem. Phys.* **7** (1939) 1103.
26. W. J. COUMANS, D. HEIKENS and S. D. SJOERDSMA, *Polymer* **21** (1980) 103.
27. D. HEIKENS, S. D. SJOERDSMA and W. J. COUMANS, *J. Mater. Sci.* **16** (1981) 429.
28. M. J. DOYLE, *ibid.* **8** (1973) 1185.
29. H. R. BROWN, *J. Polymer Sci. Polymer Phys. Ed.* **17** (1979) 1417.
30. M. AVRAMI, *J. Chem. Phys.* **8** (1940) 212.